Tubular Modular Permanent-Magnet Machines Equipped With Quasi-Halbach Magnetized Magnets—Part I: Magnetic Field Distribution, EMF, and Thrust Force

Jiabin Wang, *Senior Member, IEEE,* and David Howe

Department of Electronic and Electrical Engineering, the University of Sheffield, Sheffield S1 3JD, U.K.

This paper describes the analysis, design, and experimental characterization of three-phase tubular modular permanent-magnet machines equipped with quasi-Halbach magnetized magnets. It identifies feasible slot/pole number combinations and discusses their relative merits. It establishes an analytical expression for the open-circuit magnetic field distribution, formulated in the cylindrical coordinate system. The expression has been verified by finite-element analysis. The analytical solution allows the prediction of the thrust force and electromotive force in closed forms, and provides an effective tool for design optimization, as will be described in Part II of the paper.

***Index Terms*—Linear machines, magnetic field analysis, permanent-magnet machines.**

I. Introduction

LINEAR electromagnetic machines are being used increasingly in applications ranging from manufacturing automation [1], embedded power generation [2], [3], transportation [1], healthcare [4], [5], and household appliances [6], [7]. Whether such machines convert thrust force directly from a prime-mover (e.g., a free-piston combustion engine or Stirling engine) into electricity or provide thrust force directly to a payload, they offer numerous advantages over rotary-to-linear counterparts, notably the absence of mechanical gears and transmission systems, which results in a higher efficiency, better dynamic performance, and improved reliability. Of the various linear machine technologies and topologies, tubular permanent-magnet (PM) machines offer a high efficiency, a high power/force density, and excellent servo characteristics, which make them particularly attractive [8].

It has been shown that tubular PM machines with a Halbach magnetization, of the form illustrated in Fig. 1(a), have a number of attractive characteristics, such as a sinusoidal back-electromotive force (back-EMF) waveform, which is conducive to very low electromagnetic force ripple, and the possibility of being optimized to achieve almost zero cogging force associated with both the slotting and the finite length of the stator core [9], [10]. Since, in practice, it is relatively difficult to manufacture magnets with an ideal Halbach magnetization, a simpler form, referred to as a quasi-Halbach magnetization, as illustrated in Fig. 1(b), may be preferred. Due to the virtually "self-shielding" property of Halbach and quasi-Halbach magnetized magnets, the magnetic flux which passes through the supporting tube is relatively weak. Therefore, either a ferromagnetic or a nonmagnetic tube may be used. However, as will be shown, while a ferromagnetic tube will result in a stronger air-gap field, and therefore a better force capability, for moving-magnet tubular machines, a lightweight armature is often desirable. Therefore, a nonmagnetic supporting tube may be advantageous for many applications so as to maximize the attainable acceleration.

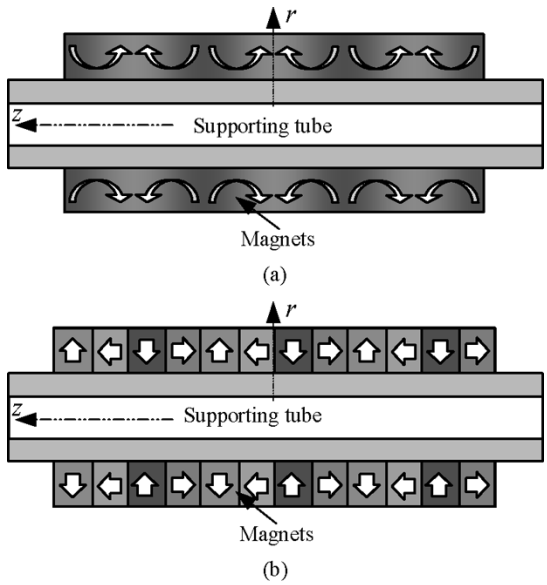

Fig. 1. Armature of tubular permanent magnet machine. (a) Halbach magnetization. (b) Quasi-Halbach magnetization.

A three-phase tubular PM machine can be wound to facilitate either brushless DC or brushless ac (BLAC) operation. A brushless dc (BLDC) machine, shown in Fig. 2(a), has two coils per pole pair per phase, displaced by 120 electrical degrees. Thus, the armature tooth pitch is two thirds of a pole pitch, and the ratio of the slot number to the pole number is 1.5. However, while the stator winding of a rotary BLDC machine has a short coil pitch, and hence a short end winding, which is conducive to a high efficiency and a high power/force density, in a tubular BLDC machine, which has no end windings, this advantage no longer exists, and the short coil pitch leads to a lower winding factor for the fundamental EMF. Hence, a

Digital Object Identifier 10.1109/TMAG.2005.854328

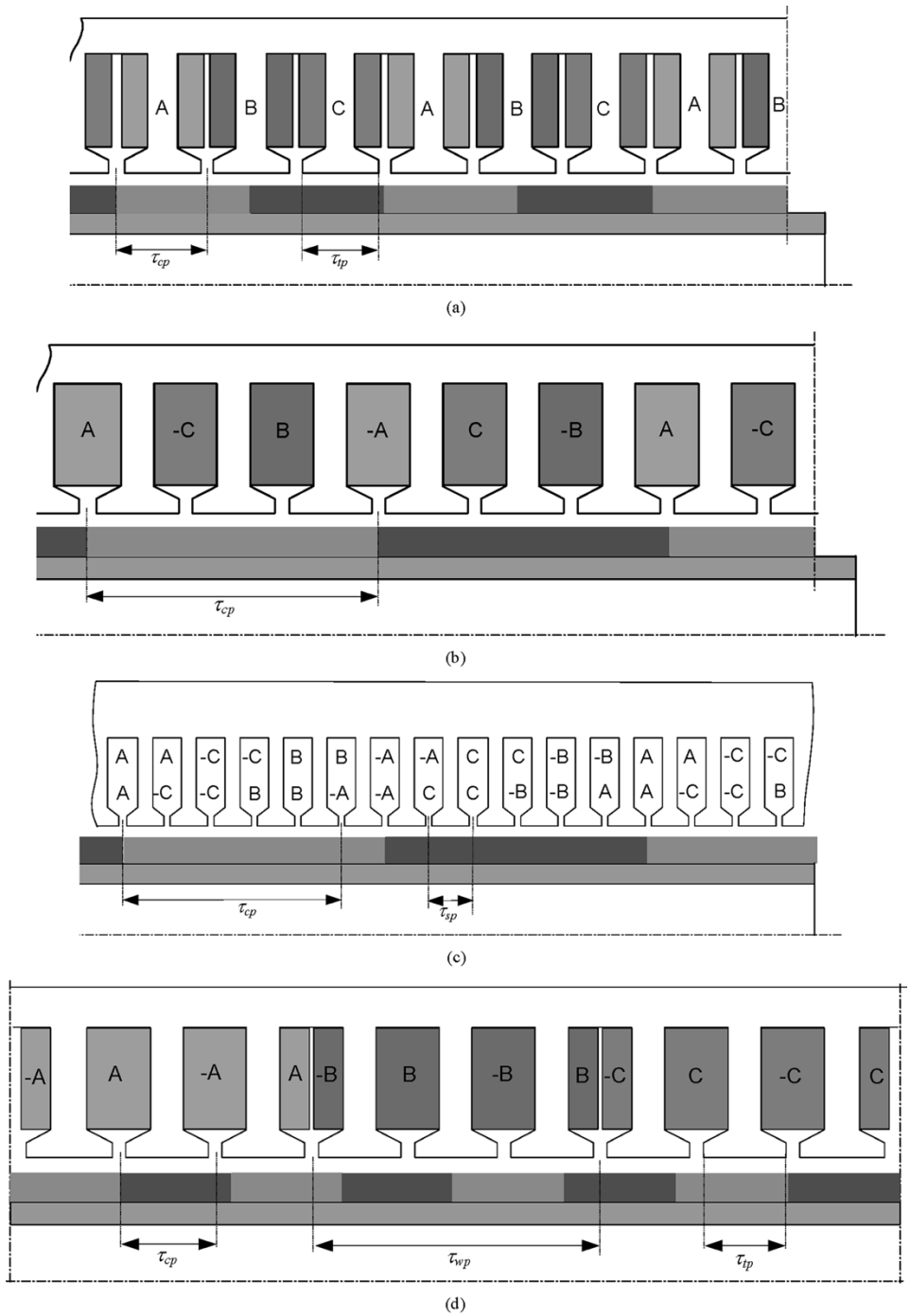

Fig. 2. Winding arrangements for three-phase tubular PM machines. (a) BLDC winding. (b) BLAC winding (one slot per pole per phase). (c) BLAC winding (short-pitched, two slots per pole per phase). (d) Modular winding (9-slot/8-pole combination).

BLDC winding is less favorable compared with a conventional three-phase BLAC winding, which has a 60° phase-spread and can be either full-pitched, with one slot per pole per phase, as in Fig. 2(b) or short-pitched, with two or more slots per pole per phase, as in Fig. 2(c). While a short-pitched winding is often used to reduce EMF harmonics and force ripple, while also providing a greater degree of freedom in selecting an appropriate ratio of slot number to pole number, primarily to minimize the cogging force, in order to eliminate low-order EMF harmonics (e.g., fifth and seventh) without a significant reduction in the winding factor, a minimum of two slots per pole per phase is required. This results in a relatively large number of slots, which can be a significant disadvantage from the manufacturing point of view, since it is then more difficult to laminate a tubular stator.

Recently, an alternative topology of three-phase tubular PM machine, referred to as modular [11], [12], has emerged which offers significant advantages over conventional tubular PM machines. Most notable is the fact that each phase winding comprises a number of concentrated coils which are disposed adjacent to each other. This results in a high winding factor and a smaller number of slots for a given number of poles, e.g., 9 slots for an 8-pole machine, as compared to 12 slots and a

minimum of 24 slots, respectively, for conventional three-phase BLDC and BLAC machines. This is not only conducive to a lower manufacturing cost, but also results in a fractional number of slots per pole. Thus, the cogging force due to the stator slots can be very small without employing skew.

The combination of a modular stator winding with a quasi-Halbach magnetized armature results in a machine with various attractive features and superior performance. This paper describes analysis and design techniques that have been developed specifically for such machines. Feasible slot/pole number combinations are identified, and various performance indicators that are pertinent to the machine design, such as the open-circuit flux linkage, the thrust force and force ripple, the iron loss, the armature reaction field and winding inductances, and the demagnetization withstand, are treated with a unified framework. These allow design optimization at a system level, taking account of both the machine and its power electronic converter.

II. Feasible Pole/Slot Number Combinations

In three-phase moving-magnet and moving-coil tubular modular PM machines, the permanent-magnet armature is usually longer than the stator in order to maximize the machine efficiency. Hence, feasible slot/pole number combinations for modular machines refer to the active part of a machine. Many feasible slot and pole combinations exist, the slot number N_s being related to the number of pole pairs p by the following:

$$N_s = 2p \pm 1 \text{ or } 2p \pm 2 \tag{1}$$

where N_s must be divisible by 3. Furthermore, for a three-phase winding, the phase shift between phases is given by

$$\theta_{\text{ps}} = \beta_s \cdot \frac{N_s}{3} \cdot \frac{180}{\beta_p} = \frac{2p\beta_p}{N_s} \cdot \left(\frac{N_s}{3} \cdot \frac{180}{\beta_p} \right) = \frac{360p}{3} \tag{2}$$

which, in electrical degrees, must equal $\pm 360k + 120$, where $k = 0, 1, 2, \ldots$ is a positive integer, β_p is the magnet pole-pitch angle, and $\beta_s = 2p\beta_p/Ns$ is the slot-pitch angle.

Table I lists all possible combinations of N_s and p derived from (1) and (2). It should be noted, from (2), that there is no feasible slot/pole number combination when p is divisible by 3. For all feasible $N_s = 2p \pm 1$ combinations, the number of slots per phase is odd. Therefore, all the coils which form one phase must be connected in series, since the EMFs which are induced in the coils are not exactly in phase. In other words, such slot/pole number combinations prevent the coils from being interconnected to form phase windings with parallel paths. As p increases, the number of coils in series also increases, and, as will be shown, the winding factor decreases, which will adversely affect the machine performance. For all feasible $N_s = 2p \pm 2$ combinations, however, the number of slots per phase is even. Therefore, the coils of each phase can be either all connected in series or connected in series/parallel groups if p is even, or connected in series/antiparallel groups if p is odd.

Thus, $N_s = 2p \pm 2$ slot/pole combinations offer greater flexibility in that the number of parallel paths may be greater than

TABLE I
Feasible Slot/Pole Number Combinations for $N_s = 2p \pm 1$ and $2p \pm 2$

	Feasible slot number, N_s	
Number of pole-pairs, p	$2p$±1	$2p$±2
1	3	-
2	3	6
4	9	6
5	9	12
7	15	12
8	15	18
10	21	18
11	21	24
13	27	24
14	27	30
16	33	30
17	33	36
19	39	36
20	39	42
22	45	42
23	45	48
…	…	…

TABLE II
Feasible Slot/Pole Combinations for Three-Phase Tubular Modular PM Machines

Number of pole-pairs, p	Number of slots, N_s
1	3
2	3, 6
3	9
4	6, 9, 12
5	9, 12, 15
6	9, 18
7	12, 15, 21
8	12, 15, 18, 24
9	27
10	18, 21, 24, 30
11	21, 24, 33
12	18, 27, 36
13	24, 27, 39
14	24, 27, 30, 42
15	27, 36, 45
16	24, 30, 33, 36, 48
17	33, 36, 51
18	27, 54
19	36, 39, 57
20	30, 36, 39, 42, 45, 48, 60

1. It will also be noted that, for a given N_s/p combination, multiplication of both p and N_s by a positive integer number results in a new feasible slot/pole combination. For example, for $N_s/p = 9/4, N_s/p = 18/8, 27/12, 36/16, \ldots$, etc., are also feasible combinations, some of which are not cited in Table I. In addition, although values of p which are integer multiples of 3 are not included in Table I, new slot/pole combinations for such pole numbers can be derived from integer multiples of the N_s/p combination for $p = 1$. In general, as the number of pole pairs increases, the number of feasible combinations of N_s and p becomes greater. For instance, when $p = 8$, there are four feasible combinations, viz. $N_s/p = 12/8, 15/8, 18/8$, and $24/8$, while when $p = 16, 5$ feasible combinations exist, viz. $N_s/p = 24/16, 30/16, 33/16, 36/16$, and $48/16$. It is evident that modular machines with an even number of pole pairs have more feasible slot/pole number combinations than those having an odd number of pole pairs. Table II summarizes all feasible slot/pole number combinations for values of p up to 20, where it will be noted that the last value of N_s in each row corresponds to

TABLE III
ADDITIONAL FEASIBLE SLOT/POLE COMBINATIONS FOR THREE-PHASE TUBULAR MODULAR PM MACHINES

Number of poles, $p/2$	Number of slots, N_s
5	6
7	6
11	12
13	12
15	18
17	18
19	18
21	18
23	24
25	24

the slot/pole number combination of a conventional PM BLDC machine.

It should also be noted that for linear PM machines, the active number of poles does not have to be an even number. Hence, additional feasible slot/pole number combinations can be derived from the combinations in Table II with an odd number of pole pairs and an even number of slots. These are listed in Table III for up to 25 active poles.

For a given number of pole pairs, different slot/pole number combinations lead to different winding factors for both the fundamental and high-order EMF harmonics, and for the armature reaction magnetomotive force distribution. Further, the cogging torque due to slotting is approximately related to the inverse of the smallest common multiple of p and N_s [13]. Thus, the choice of a particular slot/pole combination has a profound influence on the performance, demagnetization withstand capability, and noise/vibration characteristics of a machine.

III. MAGNETIC FIELD DISTRIBUTION DUE TO PERMANENT MAGNETS

In order to establish an analytical solution for the magnetic field distribution in a quasi-Halbach magnetized tubular modular machine, the following assumptions are made.

1) The axial length of the machine is infinite, so that the field distribution is axially symmetric and periodic in the z direction. However, fringing effects associated with the finite length of the armature may be considered [9].
2) The stator core is slotless, and the permeability of the iron is infinite. However, slotting effects, if present, can be taken into account by introducing a Carter coefficient [14], as has been shown in [15].

Consequently, the magnetic field analysis is confined to the airspace/winding region *I* in which the permeability is μ_0, and the permanent-magnet region *II* in which the permeability is $\mu_0\mu_r$, where μ_r is the relative recoil permeability. The governing field equations in terms of the vector magnetic potential A_θ are

$$\begin{cases} \frac{\partial}{\partial z}\left(\frac{1}{r}\frac{\partial}{\partial z}(rA_{I\theta})\right)+\frac{\partial}{\partial r}\left(\frac{1}{r}\frac{\partial}{\partial r}(rA_{I\theta})\right)=0 \\ \frac{\partial}{\partial z}\left(\frac{1}{r}\frac{\partial}{\partial z}(rA_{II\theta})\right)+\frac{\partial}{\partial r}\left(\frac{1}{r}\frac{\partial}{\partial r}(rA_{II\theta})\right)=-\mu_0\nabla\times\boldsymbol{M} \end{cases}. \tag{3}$$

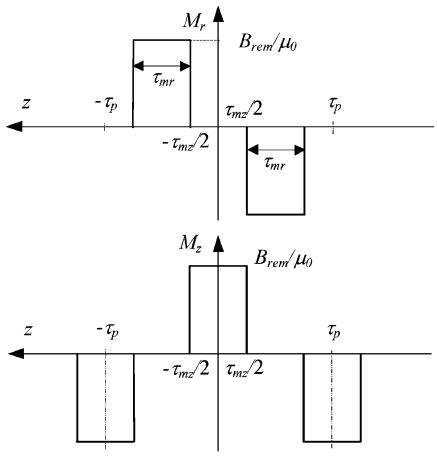

Fig. 3. Distribution of M_r and M_z.

In the cylindrical coordinate system, the magnetization $\boldsymbol{M}$ is given by

$$\boldsymbol{M}=M_r\boldsymbol{e}_r+M_z\boldsymbol{e}_z \tag{4}$$

where M_r and M_z denote the components of $\boldsymbol{M}$ in the r and z directions, respectively. Fig. 3 shows the distribution of M_r and M_z, which may be expanded into a Fourier series having the forms

$$M_r=\sum_{n=1,2,\ldots}^{\infty}M_{rn}\sin m_n z;\quad M_z=\sum_{n=1,2,\ldots}^{\infty}M_{zn}\cos m_n z \tag{5}$$

where

$$\begin{aligned} m_n&=\frac{(2n-1)\pi}{\tau_p} \\ M_{rn}&=\frac{4B_{\rm rem}}{\mu_0\tau_p m_n}\sin\frac{m_n\tau_p}{2}\sin\frac{m_n\tau_{mr}}{2}; \\ M_{zn}&=\frac{4B_{\rm rem}}{\mu_0\tau_p m_n}\sin\frac{m_n\tau_{mz}}{2} \end{aligned} \tag{6}$$

τ_p is the pole pitch, and $B_{\rm rem}$ is the remanence Thus, (3) may be further written as

$$\begin{cases} \frac{\partial}{\partial z}\left(\frac{1}{r}\frac{\partial}{\partial z}(rA_{I\theta})\right)+\frac{\partial}{\partial r}\left(\frac{1}{r}\frac{\partial}{\partial r}(rA_{I\theta})\right)=0 \\ \frac{\partial}{\partial z}\left(\frac{1}{r}\frac{\partial}{\partial z}(rA_{II\theta})\right)+\frac{\partial}{\partial r}\left(\frac{1}{r}\frac{\partial}{\partial r}(rA_{II\theta})\right)=\sum_{n=1}^{\infty}P_n\cos m_n z \end{cases} \tag{7}$$

where

$$P_n=-\frac{4B_{rm}}{\tau_p}\sin m_n\frac{\tau_p}{2}\sin m_n\frac{\tau_{mr}}{2} \tag{8}$$

The form of the solutions to (7) depends on whether the supporting tube is ferromagnetic or nonmagnetic.

A. Ferromagnetic Supporting Tube

If the permeability of the ferromagnetic supporting tube may be assumed to be infinite, only two field regions are considered, viz: the air-gap region *I* and the permanent magnet region *II*, as

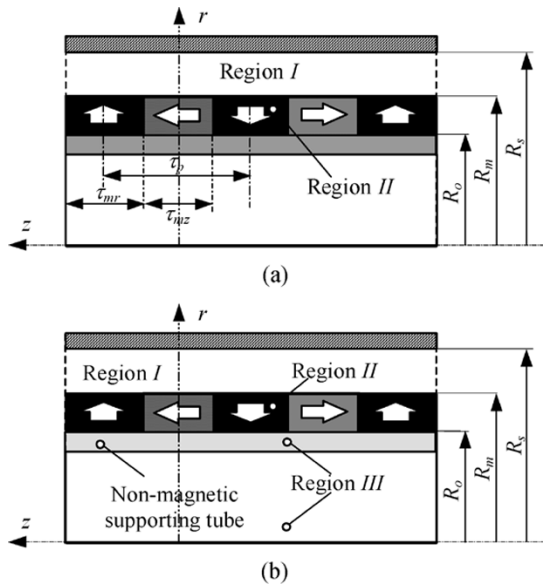

Fig. 4. Field regions. (a) Ferromagnetic tube. (b) Nonmagnetic tube.

shown in Fig. 4(a). The boundary conditions to be satisfied by (7) are

$$\begin{aligned} &B_{zI}|_{r=R_S}=0; \quad H_{zII}|_{r=R_0}=0 \\ &B_{rI}|_{r=R_m}=B_{rII}|_{r=R_m}; \quad H_{zI}|_{r=R_m}=H_{zII}|_{r=R_m}. \end{aligned} \tag{9}$$

Solving (7) subject to the boundary conditions (9) yields the following expressions for the flux density components:

$$\begin{aligned} B_{Ir}(r,z)&=\sum_{n=1,2,\ldots}^{\infty}[a_{In}BI_1(m_nr)+b_{In}BK_1(m_nr)]\sin(m_nz) \\ B_{Iz}(r,z)&=\sum_{n=1,2,\ldots}^{\infty}[a_{In}BI_0(m_nr)-b_{In}BK_0(m_nr)]\cos(m_nz) \end{aligned} \tag{10}$$

$$\begin{aligned} B_{IIr}(r,z)&=\sum_{n=1,2,\ldots}^{\infty}\{[F_{An}(m_nr)+a_{IIn}]BI_1(m_nr) \\ &\quad+[-F_{Bn}(m_nr)+b_{IIn}]BK_1(m_nr)\}\sin(m_nz) \\ B_{IIz}(r,z)&=\sum_{n=1,2,\ldots}^{\infty}\{[F_{An}(m_nr)+a_{IIn}]BI_0(m_nr) \\ &\quad-[-F_{Bn}(m_nr)+b_{IIn}]BK_0(m_nr)\}\cos(m_nz) \end{aligned} \tag{11}$$

where $BI_0(\cdot), BI_1(\cdot)$ are modified *Bessel* functions of the first kind; $BK_0(\cdot), BK_1(\cdot)$ are modified *Bessel* functions of the second kind, of order 0 and 1, respectively; and $F_{An}(\cdot), F_{Bn}(\cdot), a_{In}, b_{In}, a_{IIn}$, and b_{IIn} are defined in Appendix A.

B. Nonmagnetic Supporting Tube

When a nonmagnetic supporting tube is used, the magnetic field analysis have to encompass three regions, viz., the airspace regions *I* and *III*, and the permanent-magnet region *II*, as shown in Fig. 4(b). Although the field equations in terms of A_θ are the same as those given in (7), the boundary conditions are different, and are given by

$$\begin{aligned} &B_{zI}|_{r=R_S}=0; \quad A_{\theta III}|_{r=0}=0 \\ &B_{rI}|_{r=R_m}=B_{rII}|_{r=R_m}; \quad H_{zI}|_{r=R_m}=H_{zII}|_{r=R_m} \\ &B_{rII}|_{r=R_0}=B_{\mathrm{rIII}}|_{r=R_0}; \quad H_{zII}|_{r=R_0}=H_{zIII}|_{r=R_0}. \end{aligned} \tag{12}$$

The field solutions which satisfy the boundary conditions (12) are given by

$$\begin{aligned} B_{Ir}(r,z)&=\sum_{n=1,2,\ldots}^{\infty}[a'_{In}BI_1(m_nr)+b'_{In}BK_1(m_nr)]\sin(m_nz) \\ B_{Iz}(r,z)&=\sum_{n=1,2,\ldots}^{\infty}[a'_{In}BI_0(m_nr)-b'_{In}BK_0(m_nr)]\cos(m_nz) \end{aligned} \tag{13}$$

$$\begin{aligned} B_{IIr}(r,z)&=\sum_{n=1,2,\ldots}^{\infty}\{[F_{An}(m_nr)+a'_{IIn}]BI_1(m_nr) \\ &\quad+[-F_{Bn}(m_nr)+b'_{IIn}]BK_1(m_nr)\}\sin(m_nz) \\ B_{IIz}(r,z)&=\sum_{n=1,2,\ldots}^{\infty}\{[F_{An}(m_nr)+a'_{IIn}]BI_0(m_nr) \\ &\quad-[-F_{Bn}(m_nr)+b'_{IIn}]BK_0(m_nr)\}\cos(m_nz) \end{aligned} \tag{14}$$

$$\begin{aligned} B_{IIIr}(r,z)&=\sum_{n=1,2,\ldots}^{\infty}[a'_{IIIn}BI_1(m_nr)]\sin(m_nz) \\ B_{IIIz}(r,z)&=\sum_{n=1,2,\ldots}^{\infty}[a'_{IIIn}BI_0(m_nr)]\cos(m_nz) \end{aligned} \tag{15}$$

where the definitions of $a'_{In}, b'_{In}, a'_{IIn}, b'_{IIn}$, and a'_{IIIn} are given in Appendix B.

TABLE IV
DESIGN PARAMETERS OF TUBULAR MODULAR PM MACHINE (m)

R_s	R_m	R_0	τ_p	τ_{mr}	τ_{mz}
0.0255	0.0245	0.0195	0.01	0.006	0.004

C. Comparison With Finite-Element Analysis

The main design parameters of a three-phase tubular modular PM machine, for which analytical field solutions have been obtained, are given in Table IV. The magnets are sintered NdFeB, for which $B_{\mathrm{rem}} = 1.15$ T and $\mu_r = 1.05$. The analytical field distribution has been validated by finite-element calculation of the radial and axial variations of the radial and axial flux density components in the air-gap and winding regions.

The finite-element solution was obtained by applying a periodic boundary condition at the axial boundaries $z = \pm\tau_p$ and imposing the natural Neumann boundary condition at the surface of the ferromagnetic stator core and the surface of the supporting tube, if it is ferromagnetic. Fig. 5 compares numerically and analytically calculated distributions of the axial and radial flux density components, B_{zI}, and B_{rI}, as functions of the axial position z at a constant radius, $r = 0.025$ m, with a

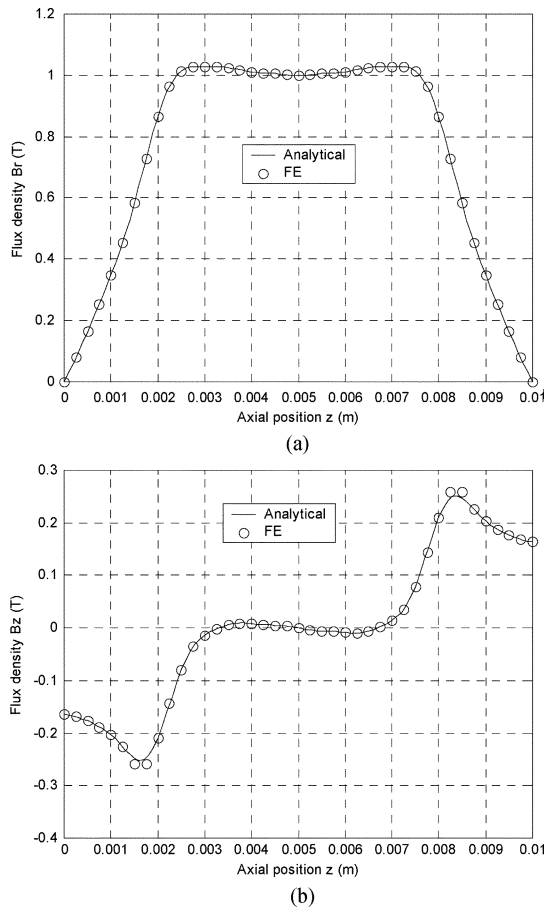

Fig. 5. Comparion of radial and axial flux density components at $r = 0.025$ m. (a) Variation of B_r as a function of z; (b) variation of B_z as a function of z.

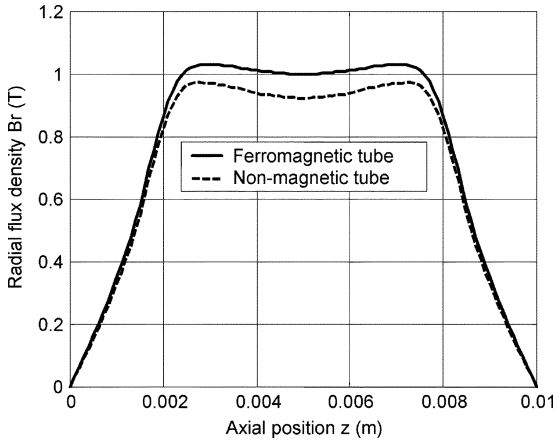

Fig. 6. Comparison of radial flux density components at $r = 0.025$ m.

magnetic supporting tube. It will be seen that the analytical solutions agree extremely well with the finite-element predictions, the main cause of any discrepancies being due to discretization errors in regions where the components of flux density vary rapidly.

Fig. 6 compares the radial flux density component which results with ferromagnetic and nonmagnetic supporting tubes. As can be observed, the ferromagnetic tube results in a stronger air-gap flux density, and, hence, a higher force capability.

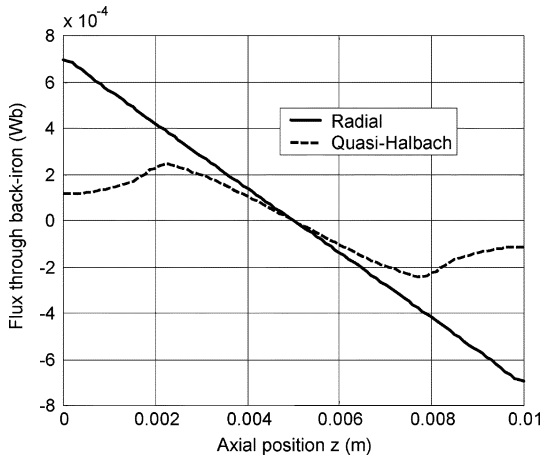

Fig. 7. Comparison of flux passing through ferromagnetic supporting tube.

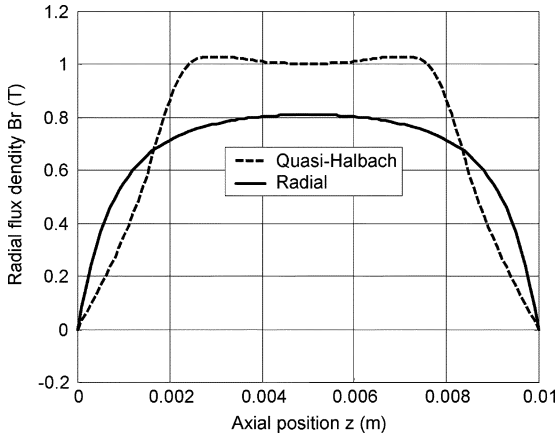

Fig. 8. Comparison of radial flux density at $r = 0.025$ m.

TABLE V
HARMONIC COMPONENTS OF RADIAL FLUX DENSITY (T)

Harmonic order	Radially magnetized	Quasi-Halbach magnetized
1	0.956	1.164
3	0.198	0.128
5	0.076	0.076
7	0.037	0.047

In order to illustrate the benefit of employing the quasi-Halbach magnetization as compared to a radial magnetization [15], Fig. 7 compares the flux which passes through the ferromagnetic tube as a function of axial position, while Fig. 8 compares the radial flux density component in the air gap at $r = 0.025$ m, a comparison of the harmonic components being given in Table V. As can be seen, while the fifth and seventh harmonic components are almost identical, with the quasi-Halbach magnetization the fundamental component is 20% higher and the third harmonic is 36% lower than the corresponding components which result with the radial magnetization. Further, the peak flux which results in the ferromagnetic tube with the quasi-Halbach magnetization is $\sim$3 times lower than that with the radial magnetization. Consequently, its radial thickness can be much lower. This is particularly important for moving-magnet machines, as a lower mass results in a higher acceleration capability.

IV. Flux Linkage, EMF, and Thrust Force

For tubular modular PM machines with a slotted stator, the influence of slotting may be accounted for by introducing a Carter coefficient, K_c, given by [14], [15]:

$$K_C = \frac{\tau_{\rm sp}}{\tau_{\rm sp} - \gamma g'} \tag{16}$$

where $g' = g + h_m/\mu_r, \tau_{\rm sp}$ is the stator slot-pitch, g is the air-gap length, μ_r is the relative recoil permeability of the permanent magnets, and h_m is their radial thickness, and the slotting factor γ is given by

$$\gamma = \frac{4}{\pi}\left\{\frac{b_0}{2g'}\tan^{-1}\left(\frac{b_0}{2g'}\right) - \ln\sqrt{1+\left(\frac{b_0}{2g'}\right)^2}\right\} \tag{17}$$

where b_0 is the width of the stator slot openings. Therefore, the effective air-gap length g_e and the equivalent stator bore radius $R_{\rm se}$ are given, respectively, by

$$g_e = g + (K_c - 1)g' \tag{18}$$

$$R_{\rm se} = R_m + g_e \tag{19}$$

where R_m is the outer radius of the magnets. It has been shown in [15] that the flux linkage of a stator coil can be obtained by integrating the radial flux density component at $r = R_{\rm se}$ over the coil pitch. The total flux linkage of a phase winding is therefore the sum of the flux linkages in all the coils which are connected in series, and is given by

$$\Psi_{\rm pw} = \sum_{n=1,2,\ldots}^{\infty} \Phi_{np}\cos m_n(z - \tau_{\rm wp}/2) \tag{20}$$

where

$$\Phi_{\rm np} = \frac{2\pi N_{\rm wp}K_{dpn}}{m_n}K_{rn} \tag{21}$$

in which $N_{\rm wp}$ is the number of series turns per phase and $\tau_{\rm wp}$ is the axial span of the phase winding. K_{dpn} is defined as the winding factor of the $(2n-1)$th harmonic, and K_{rn} is the coefficient related to the $(2n-1)$th harmonic in the radial field distribution, and is given by

$$K_{rn} = \begin{cases} R_{\rm se}[a_{In}BI_1(m_nR_{\rm se}) + b_{In}BK_1(m_nR_{\rm se})] \\ \quad \text{Ferromagnetic tube} \\ R_{\rm se}[a'_{In}BI_1(m_nR_{\rm se}) + b'_{In}BK_1(m_nR_{\rm se})] \\ \quad \text{Nonmagnetic tube} \end{cases}. \tag{22}$$

The winding factor K_{dpn} is the product of the pitch factor K_{pn} and the distribution factor K_{dn}. The pitch factor is related to the coil-pitch $\tau_{\rm cp}$ by

$$K_{pn} = \sin\left(\frac{m_n\tau_{\rm cp}}{2}\right). \tag{23}$$

Since the coils in each phase of a modular winding are displaced by

$$\theta_d = \text{abs}(\tau_p - \tau_{\rm cp})\frac{\pi}{\tau_p} \tag{24}$$

the distribution factor K_{dn} of a phase winding having $N_{\rm sp}$ series connected coils is given by

$$K_{dn} = \frac{\sin\left(\dfrac{N_{sp}(2n-1)\theta_d}{2}\right)}{N_{sp}\sin\left(\dfrac{(2n-1)\theta_d}{2}\right)}. \tag{25}$$

The no-load flux that passes through a stator tooth can be similarly calculated by integrating the radial flux density component at $r = R_{\rm se}$ over the tooth pitch width $\tau_{\rm tp}$, and the flux in the stator back-iron and the supporting tube can be evaluated using the formulas given in [16].

The induced EMF in each phase winding is given by

$$e_{\rm pw} = -\frac{d\Psi_{\rm pw}}{dt} = -v\sum_{n=1,2,\ldots}^{\infty} K_{En}\sin m_n\left(z - \frac{\tau_{\rm wp}}{2}\right) \tag{26}$$

where v is the linear velocity of the armature, and K_{En} is the EMF constant of the $(2n-1)$th harmonic, and is given by

$$K_{En} = 2\pi N_{\rm wp}K_{dpn}K_{rn}. \tag{27}$$

It can be shown [16] that the instantaneous force of the machine, when the three phases are excited with balanced sinusoidally time-varying currents which are in phase with the phase EMFs, is given by

$$F = F_1 + \sum_{\substack{n=3k+1\\k=1,2\ldots}}^{\infty} F_{n1}\cos\left[(2n-2)\left(\frac{\pi z}{\tau_p}\right)\right] + \sum_{\substack{n=3k+3\\k=0,1,2\ldots}}^{\infty} F_{n3}\cos\left[(2n-5)\left(\frac{\pi z}{\tau_p}\right)\right] \tag{28}$$

where F_1, F_{n1}, and F_{n3} are given by

$$\begin{aligned} F_1 &= -\sqrt{2}K_1\frac{3}{2}J_{\rm rms}P_f \\ F_{n1} &= \sqrt{2}J_{\rm rms}\frac{3}{2}K_n(-1)^k, \quad n = 3k+1, \quad k = 1,2,\ldots. \\ F_{n3} &= \sqrt{2}J_{\rm rms}\frac{3}{2}K_n(-1)^{k+1}, \quad n = 3k+3, \quad k = 0,1,2,\ldots \end{aligned} \tag{29}$$

in which $K_n = 4\pi pK_{dpn}K_{rn}S_{\rm AP}$, $J_{\rm rms}$ is the rms current density, P_f is the copper packing factor, and $S_{\rm AP}$ is the total slot area per pole. As will be evident from (29), the force ripple due

to triple harmonics in the radial air-gap field distribution is zero. The normalized total force ripple is therefore given by

$$\text{TFR} = \frac{\sqrt{\sum_{n=3} F_n^2}}{F_1} = \frac{\sqrt{\sum_{n=3} K_n^2}}{K_1}, \quad n \neq 3k+2, \quad k = 0,1,2,\ldots. \tag{30}$$

V. Conclusion

Feasible slot/pole number combinations for three-phase tubular modular PM machines have been derived, and their relative merits have been evaluated. An analytical expression has been established for the open-circuit magnetic field distribution which results with a quasi-Halbach magnetized armature, for both a nonmagnetic and ferromagnetic supporting tube, and this has been verified by finite-element analysis. It has been shown that, compared with a radial magnetization, a quasi-Halbach magnetization results in a lower harmonic content in the airgap field, and a lower flux in the ferromagnetic tube on which the magnets may be mounted. These features are very attractive for applications that require a low force ripple and a high acceleration capability.

Appendix

A. Definition of $FA_n(\cdot), FB_n(\cdot), a_{In}, b_{In}, a_{IIn}$, and b_{IIn}

Let

$$\begin{aligned}
c_{1n} &= BI_0(m_n R_s); \quad c_{2n} = BK_0(m_n R_s);\\
c_{3n} &= BI_1(m_n R_m); \quad c_{4n} = BK_1(m_n R_m);\\
c_{5n} &= BI_0(m_n R_m); \quad c_{6n} = BK_0(m_n R_m);\\
c_{7n} &= BI_1(m_n R_0); \quad c_{8n} = BK_1(m_n R_0);\\
c_{9n} &= BI_0(m_n R_0); \quad c_{10n} = BK_0(m_n R_0)
\end{aligned}$$

$$F_{An}(m_n r) = \frac{P_n}{m_n} \int_{m_n R_0}^{m_n r} \frac{BK_1(x)dx}{BI_1(x)BK_0(x) + BK_1(x)BI_0(x)}$$

$$F_{Bn}(m_n r) = \frac{P_n}{m_n} \int_{m_n R_0}^{m_n r} \frac{BI_1(x)dx}{BI_1(x)BK_0(x) + BK_1(x)BI_0(x)}$$

$$B_n = \frac{4B_{\text{rem}}}{\mu_r \tau_p m_n} \sin\frac{m_n \tau_{mz}}{2}.$$

Then, A_{In}, B_{In}, A_{IIn}, and B_{IIn} are solutions of the following linear equations:

$$\begin{bmatrix} 1 & -\frac{c_{2n}}{c_{4n}} & 0 & 0 \\ \frac{c_{3n}}{c_{1n}} & 1 & \frac{c_{3n}}{c_{5n}} & \frac{c_{4n}}{c_{10n}} \\ \frac{c_{5n}}{c_{1n}} & -\frac{c_{6n}}{c_{4n}} & 1 & -\frac{c_{6n}}{\mu_r c_{10n}} \\ 0 & 0 & -\frac{\mu_r c_{9n}}{c_{5n}} & 1 \end{bmatrix} \begin{bmatrix} A_{In} \\ B_{In} \\ A_{IIn} \\ B_{IIn} \end{bmatrix} = \begin{bmatrix} 0 \\ c_{3n}F_{An}(m_nR_m) - c_{4n}F_{Bn}(m_nR_m) \\ \frac{1}{\mu_r}[c_{5n}F_{An}(m_nR_m) + c_{6n}F_{Bn}(m_nR_m)] - B_n \\ \mu_r B_n \end{bmatrix}$$

a_{In}, b_{In}, a_{IIn}, and b_{IIn} are then given by

$$a_{In} = \frac{A_{In}}{c_{1n}}; \quad b_{In} = \frac{B_{In}}{c_{4n}}; \quad a_{IIn} = -\mu_r \frac{A_{IIn}}{c_{5n}}; \quad b_{IIn} = -\frac{B_{IIn}}{c_{10n}}.$$

B. Definition of $a'_{In}, b'_{In}, a'_{IIn}, b'_{IIn}$, and a'_{IIIn}

Let $A'_{In}, B'_{In}, A'_{IIn}, B'_{IIn}$, and A'_{IIIn} be solutions of the following linear equations:

$$\begin{bmatrix} 1 & -\frac{c_{2n}}{c_{4n}} & 0 & 0 & 0 \\ \frac{c_{3n}}{c_{1n}} & 1 & \frac{\mu_r c_{3n}}{c_{5n}} & -\frac{c_{4n}}{c_{8n}} & 0 \\ \frac{c_{5n}}{c_{1n}} & -\frac{c_{6n}}{c_{4n}} & 1 & \frac{c_{6n}}{\mu_r c_{8n}} & 0 \\ 0 & 0 & -\frac{\mu_r c_{7n}}{c_{5n}} & 1 & \frac{c_{7n}}{c_{9n}} \\ 0 & 0 & -\frac{c_{9n}}{c_{5n}} & -\frac{c_{10n}}{\mu_r c_{8n}} & 1 \end{bmatrix} \begin{bmatrix} A'_{In} \\ B'_{In} \\ A'_{IIn} \\ B'_{IIn} \\ A'_{IIIn} \end{bmatrix} = \begin{bmatrix} 0 \\ c_{3n}F_{An}(m_nR_m) - c_{4n}F_{Bn}(m_nR_m) \\ \frac{1}{\mu_r}[c_{5n}F_{An}(m_nR_m) + c_{6n}F_{Bn}(m_nR_m)] - B_n \\ 0 \\ B_n \end{bmatrix}.$$

Then, $a'_{In}, b'_{In}, a'_{IIn}, b'_{IIn}$, and a'_{IIIn} are given by

$$a'_{In} = \frac{A'_{In}}{c_{1n}}; \quad b'_{In} = \frac{B'_{In}}{c_{4n}}; \quad a'_{IIn} = -\frac{\mu_r A'_{IIn}}{c_{5n}}; \quad b'_{IIn} = \frac{B'_{IIn}}{c_{8n}}; \quad a'_{IIIn} = -\frac{A'_{IIIn}}{c_{9n}}.$$

References

[1] E. Masada, "Linear drives for industrial applications in Japan—History, existing state, and future prospect," in *Proc. LDIA'95*, Japan, 1995, pp. 9–12.

[2] M. A. White, K. Colenbrander, R. W. Olan, and L. B. Penswick, "Generators that won't wear out," *Mech. Eng.*, vol. 118, no. 2, pp. 92–96, 1996.

[3] W. R. Cawthorne, P. Famouri, J. Chen, N. N. Clarke, T. I. McDaniel, R. J. Atkinson, S. Nandkumar, C. M. Atkinson, and S. Petreanu, "Development of a linear alternator-engine for hybrid electric vehicle applications," *IEEE Trans. Veh. Technol.*, vol. 48, no. 6, pp. 1797–1802, Nov. 1999.

[4] R. E. Clark, D. S. Smith, P. H. Mellor, and D. Howe, "Design optimization of moving-magnet actuators for reciprocating electro-mechanical systems," *IEEE Trans. Magn.*, vol. 31, no. 6, pp. 3746–48, Nov. 1995.

[5] M. Watada, K. Yanashima, Y. Oishi, and D. Ebihara, "Improvement on characteristics of linear oscillatory actuator for artificial hearts," *IEEE Trans. Magn.*, vol. 29, no. 6, pp. 3361–63, Nov. 1993.

[6] K. Park, E. P. Hong, and K. H. Lee, "Development of a linear motor for compressors of household refrigerators," in *Proc. LDIA'2001*, Nagano, Japan, 2001, pp. 283–286.

[7] M. Utsuno, M. Takai, T. Yaegashi, T. Mizuno, H. Yamamoto, K. Shibuya, and H. Yamada, "Efficiency characteristics of a linear oscillatory actuator under simulated compressor load," in *Proc. LDIA'2001*, Nagano, Japan, 2001, pp. 264–267.

[8] J. F. Eastham, "Novel synchronous machines: Linear and disc," *Proc. Inst. Elect. Eng.*, vol. B-137, pp. 49–58, 1990.

[9] J. Wang, D. Howe, and G. W. Jewell, "Fringing in tubular permanent magnet machines: Part I—Magnetic field distribution, flux-linkage, and thrust force," *IEEE Trans. Magn.*, vol. 39, no. 6, pp. 3507–3516, Nov. 2003.

[10] ——, "Fringing in tubular permanent magnet machines: Part II—Cogging force and its minimization," *IEEE Trans. Magn.*, vol. 39, no. 6, pp. 3517–3522, Nov. 2003.

[11] M. Inoue, J. Wang, and D. Howe, "Influence of slot openings in tubular modular permanent magnet machines," in *Proc. LDIA*, Birmingham, U.K., Sep. 2003, pp. 383–386.

[12] Y. Amara, J. Wang, and D. Howe, "Eddy current loss in tubular modular permanent magnet machines," presented at the Int. Conf. Electrical Machines (ICEM 2004), Cracow, Poland, 2004, Paper 193.
[13] Z. Q. Zhu and D. Howe, "Influence of design parameters on cogging torque in permanent magnet machines," *IEEE Trans. Energy Convers.*, vol. 15, no. 4, pp. 407–412, Dec. 2000.
[14] Q. Gu and H. Gao, "Effect of slotting in PM electrical machines," *Elect. Mach. Power Syst.*, vol. 10, no. 2, pp. 273–284, 1985.
[15] J. Wang, G. W. Jewell, and D. Howe, "A general framework for the analysis and design of tubular linear permanent magnet machines," *IEEE Trans. Magn.*, vol. 35, no. 3, pp. 1986–2000, May 1999.
[16] J. Wang and D. Howe, "Design optimization of radially magnetized, iron-cored, tubular permanent magnet machines and drive systems," *IEEE Trans. Magn.*, vol. 40, no. 5, pp. 3262–3277, Sep. 2004.

Manuscript received March 23, 2005; revised June 10, 2005.

Jiabin Wang (SM'03) was born in Jiangsu Province, China, in 1958. He received the B.Eng. and M.Eng. degrees in electrical and electronic engineering from Jiangsu University of Science and Technology, Zhengjiang, China, in 1982 and 1986, respectively, and the Ph.D. degree in electrical and electronic engineering from the University of East London, London, U.K., in 1996.

Currently, he is a Senior Lecturer at the University of Sheffield, Sheffield, U.K. From 1986 to 1991, he was with the Department of Electrical Engineering at Jiangsu University of Science and Technology, where he was appointed a Lecturer in 1987 and an Associated Professor in 1990. He was a Postdoctoral Research Associate at the University of Sheffield, Sheffield, U.K., from 1996 to 1997, and a Senior Lecturer at the University of East London from 1998 to 2001. His research interests range from motion control to electromagnetic devices and drive systems.

David Howe received the B.Tech. and M.Sc. degrees in electrical power engineering from the University of Bradford, Bradford, U.K., in 1966 and 1967, respectively, and the Ph.D. degree in electrical power engineering from the University of Southampton, Southampton, U.K.

Currently, he is a Professor of Electrical Engineering at the University of Sheffield, Sheffield, U.K., where he heads the Electrical Machines and Drives Research Group. He has held academic posts at Brunel University, London, U.K., and Southampton University, and spent a period in industry with NEI Parsons Ltd., Newcastle-Upon-Tyne, U.K., working on electromagnetic problems related to turbogenerators. His research activities span all facets of controlled electrical drive systems with particular emphasis on permanent-magnet-excited machines.

Dr. Howe is a Fellow of the Institution of Electrical Engineers, U.K., and Fellow of the Royal Academy of Engineering, U.K.